Dear reviewer:

Thank you very much for your careful review and constructive suggestions with regard to this manuscript. We appreciate for Reviewer's work earnestly, and hope that the corrections will meet with approval. Please find below our detailed responses to reviewer's question and comments.

Referee #3

The paper presents a method to estimate refractive indices for both fine and coarse mode particles. The retrieval from AERONET assumes size-independent refractive index. The paper assumes that the imaginary part of refractive index has no spectral variation except at 440 nm, while real part of of refractive index has no no spectral variation from 440 - 1020 nm. The size parameters are then derived by fitting lognormal distributions to the inverted size-bin data from AERONET. Mie calculation is conducted to find the sets of both fine and coarse aerosols refractive indices that give the best agreement with AOD and absorbing AOD from AERONET. Overall, the math in this paper is sound. The results presented for Beijing are interesting. The paper needs more justification of its assumptions and more validation.

1) The assumption that the imaginary part of refractive index has no spectral variation except at 440 nm, while real part of of refractive index has no no spectral variation from 440 - 1020 nm. Is this assumption consistent with the assumption in AERONET's inversion algorithm?

Response: Firstly, this assumption is only set to output (CRI of separated fine & coarse modes) of this work, instead of inputs (i.e. the AERONET's inversion products still keep their spectral variation). The objective of this work (separating CRI of fine & coarse modes) focuses on improving the inference of aerosol component information. Figure 1 shows the real parts (n) of the majority of aerosol components are quite constant from UV to near infrared spectral region, and imaginary parts show a significant spectral variation at short wavelengths (e.g. 440nm). This explains our basic consideration on the assumption of the spectral behaviors of output CRIs. In addition, the AERONET algorithm paper stated the similar consideration (Dubovik & King, JGR, 2000):

"*Spectral variability is usually* ***not expected for both real and imaginary parts*** *of the aerosol particle refractive index. For example, the widely cited paper by Shettle and Fenn [1979] shows practically wavelength-independent complex refractive indices in the spectral interval of interest (440-1020 nm) for the materials typically composing atmospheric aerosols. Similarly, aerosol models by Tanre et al. [1999] assume single constant values of complex refractive index for the spectral interval considered."*

Secondly, we think that this assumption is not in confliction with AERONET's

algorithm. The AERONET inversion algorithm assumes identical real and imaginary parts of the refractive indices for both fine and coarse modes coincidently, but allowing independent values at each wavelength (440, 675, 870 and 1020nm). This is mainly to deal with the mixture of mode/components, which can be seen (note: there, "aerosol particles" means mixture of fine & coarse modes) in their paper (Dubovik & King, JGR, 2000):

"*However, in the scientific literature there are multiple indications of possible spectral selectivity of the refractive index for aerosol particles [e.g., Ackerman and Toon, 1981; Patterson and McMahon, 1984; Horvath, 1993; Dubovik et al., 1998b, Yumasoe et al., 1998]. Therefore we constrain the spectral variability of the retrieved complex refractive index to some practically reasonable ranges rather than to any particular model of the atmospheric aerosol."*

2) In cases/locations when AERONET's inversion shows dominant fraction (~100%) of fine-mode aerosols, its retrieved index of refraction should be considered as appropriate for fine-mode aerosols. The same holds true when aerosols are dominated by coarse particles. There are AERONET sites close to Gobi desert. It will be valuable to look at several cases where dust particles are transported from Gobi desert to Beijing, and compare the retrieved index of refraction for coarse mode in Beijing with that directly retrieved from AERONET site close to the dust source.

Response: According to the Reviewer's comments, we choose a dust event period from Apr. 17-19 2017 both at Beijing site and Dalanzadgad site close to Gobi desert in Mongolia (Fig. S1a). The dust aerosol in Beijing transported from Dalanzadgad site can be seen clearly in Fig 1b, simulated by HYSPLIT model reached Apr. 20, 2017. The high concentrations of volume particle size distributions in coarse mode (Fig. S2) are similar at Dalanzadgad and Beijing site. It is indicate that the similar properties of dust can be observed at both Beijing and Dalanzadgad sites. Fig. S3(a) and (b) shows a fairly good consistency of the real parts (n) at Dalanzadgad from AERONET and the retrievals for coarse mode in Beijing from our algorithm and close to 1.6, although the observed time is not an exact match. But the imaginary parts do not agree each other. It can be explained by the variation of transported aerosol properties. In addition, some uncertainties can be involved in analysis and retrieval because the AERONET Lev 1.5 data is used in this part. Particularly, the strong absorption (large k) in Dalanzadgad site on Apr. 17 is inveracious.

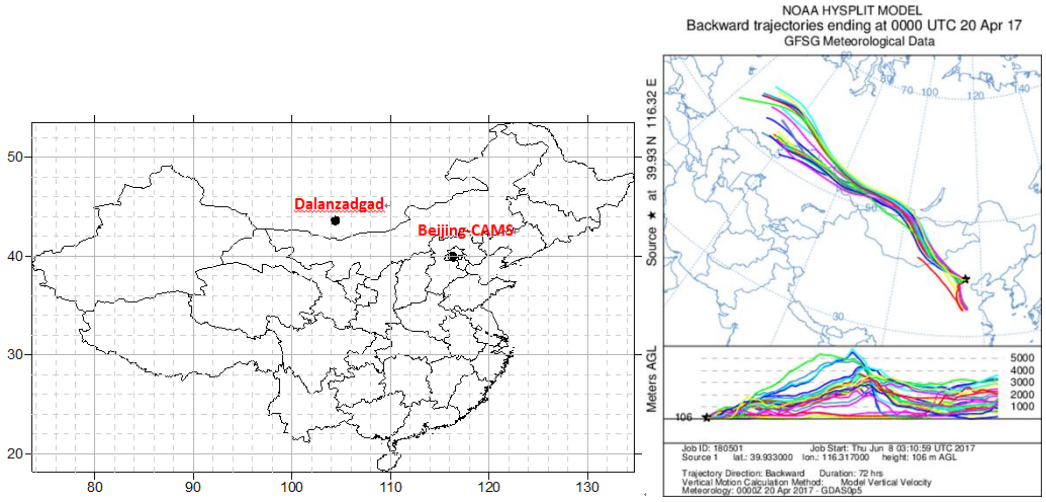

Fig. S1 (a) Map of site locations; (b) backward trajectory on Apr. 17-19, 2017

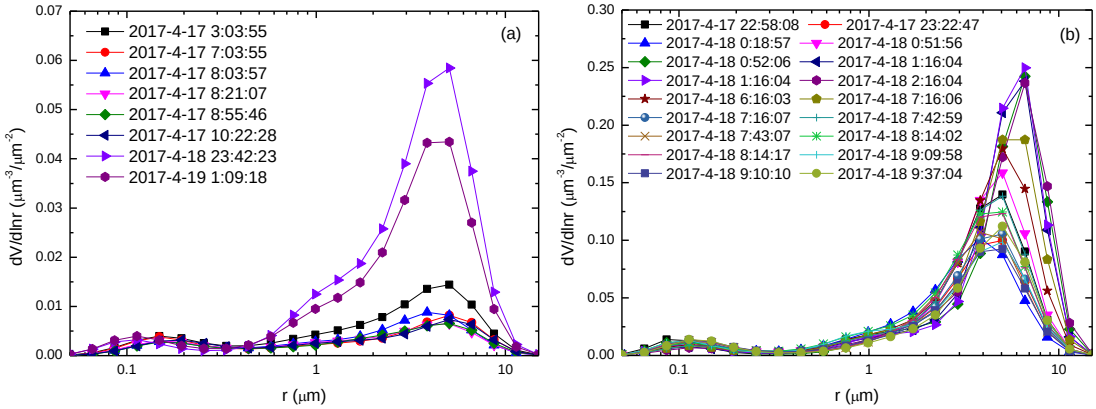

Fig. S2 volume particle size distributions of (a) Dalanzadgad and (b) Beijing site during Apr. 17-19, 2017.

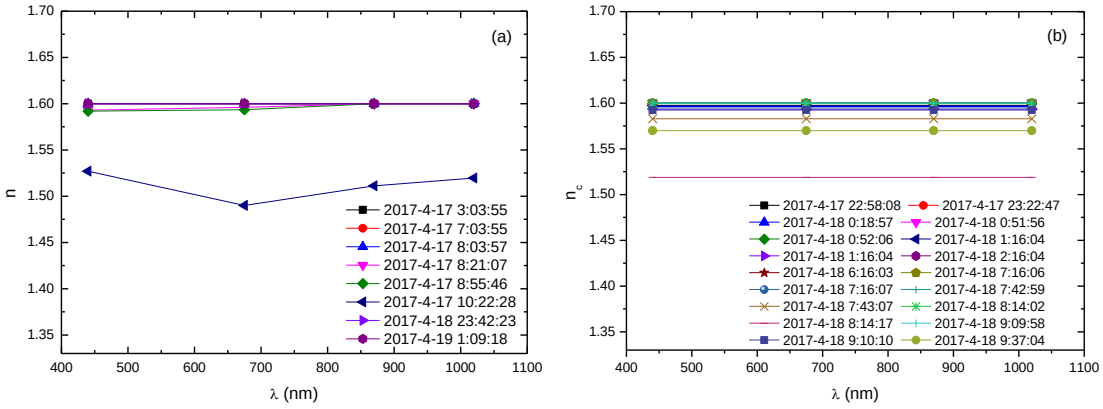

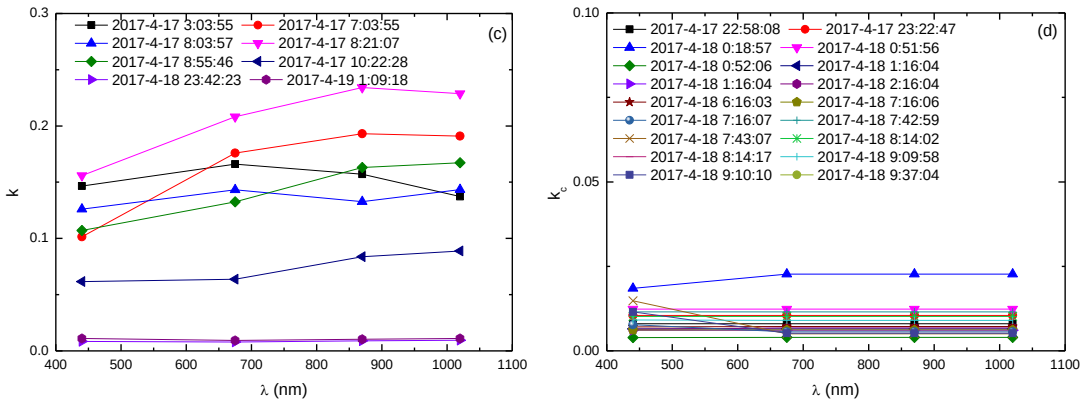

Fig. S3 The comparison of CRI from AERONET at Dalanzadgad site (a, c) and retrieved one in coarse mode at Beijing site (b, d).

To further detect the accuracy of coarse mode, additional three typical dust aerosol model (Dubovik et al., 2002) are employed and combined with the fine-mode WS and BB (Table 1). As the Table S1 shows, The error of real part in coarse mode is lower than 0.1, and the retrieved imaginary part of CRI in coarse mode is more accurate with the error of less than 0.003 except for the biomass burning model.

Table S1. The retrieved errors of typical dust aerosol models.

Aerosol model	Input CRI in coarse mode			Error in coarse mode		
	n_c	$k_{c,440}$	k_c	n_c	$k_{c,440}$	k_c
WS	1.55	0.0025	0.001	-0.091	0.000	0.003
	1.56	0.0029	0.001	-0.099	0.000	0.003
	1.48	0.0025	0.0006	-0.033	0.000	0.003
BB	1.55	0.0025	0.001	-0.013	0.018	0.022
	1.56	0.0029	0.001	-0.022	0.018	0.021
	1.48	0.0025	0.0006	0.054	0.019	0.022
DU	1.55	0.0025	0.001	-0.008	0.000	0.000
	1.56	0.0029	0.001	-0.009	0.000	0.000
	1.48	0.0025	0.0006	-0.010	0.000	0.000

Dubovik O., Holben B., Eck T. F., Smirnov A., Kaufman Y. J., King M. D., Tanre D. and Slutsker I. (2002), Variability of absorption and optical properties of key aerosol types observed in worldwide locations, Journal of the atmospheric sciences, 59, 590-608.

Referee #4

The Authors present a method for the separate estimation of the aerosol refractive index from AERONET data. First they fit AERONET aerosol size distribution to a multimodal log-normal distribution, then they group the modes of the fitted log-normal distribution into a "fine" and a "coarse" mode, and then

they proceed to the estimate of the refractive index of each mode by an iterative fitting AERONET total and absorption AOTs to Mie forward calculations. The proposed method looks fine to me. The steps of the procedure are well identified, the underlying assumptions are clearly stated and so are the limitations of the method (e.g., not taking the possibility of nonspherical particles into account). The validation on synthetic data, instead, looks a bit shallow, because the Authors only test three configurations, in which three realistic fine mode aerosol types (water-soluble, biomass burning and dust) are combined with a "default" coarse mode with refractive index 1.53+i0.008: in this section I would have been curious to see tests with more combinations of aerosol parameters. Anyway, in the last section of the paper the Authors also make the effort of applying their method to real AERONET measurements taken at Beijing, and they show that their separate retrieval allows a reasonable physical interpretation (which is probably the best possible "validation" of a refractive index retrieval, given that independent correlative measurements of this parameter are very difficult to obtain. and even an objective definition of the refractive index of a mixture of aerosol components is problematic in itself). Furthermore, the Authors show that their multicomponent refractive index retrievals fit AERONET AOTs quite well. In view of this, I think this paper can be published with minor revisions. I would recommend, though, a proofreading by a native English speaker, because the quality of the written English looks below par in some parts of the manuscript. Below are some suggestions for the modification of some unclear statements, and some other minor comments.

MINOR COMMENTS

(1) P1, L4-5. I would suggest to change "…based on AERONET aerosol products, including" etc., with "…based on AERONET volume particle size distribution" etc.

Response: We have corrected according to the Reviewer's comments.
"This paper establishes a method to separate CRIs of fine and coarse particles based on AERONET volume particle size distribution (VPSD), aerosol optical depth (AOD) and absorbing AOD."

(2) P1, L5-6. The sentence "The method … simultaneously" is a bit unclear. Consider removing it or rephrasing with something like "The method consists of two steps. First a multimodal log-normal distribution that best approximates the AERONET VPSD is found. Then the fine and coarse mode CRIs are found by iterative fitting of AERONET AODs to Mie calculations."

Response: We have corrected according to the Reviewer's comments.
"The method consists of two steps. First a multimodal log-normal distribution that

best approximates the AERONET VPSD is found. Then the fine and coarse mode CRIs are found by iterative fitting of AERONET AODs to Mie calculations."

(3) P2, L8-9. I do not understand what the last two sentences mean. Especially the last one ("Raul and Chazette etc.").

Response: We have corrected the sentences in the manuscript.
"In addition, Li et al. (2006) further added the polarized sky radiance measurements to the inversion algorithm in order to better constrain AERONET CRI retrievals. The Lidar measurements are also used to obtain CRI of aerosols within planetary boundary layer (Raut and Chazette, 2007)."

(4) P2, L17. Change "There are only few studies … attempted..." to "Only a few studies … attempted...". Furthermore, Wu et al. (2015) does not describe retrieval from ground-based measurements. It describes retrievals from airborne measurements.

Response: We have corrected according to the Reviewer's comments.
"Only few studies (e.g. Xu et al., 2015; Wu et al., 2015) attempted to retrieve CRI of both fine and coarse modes simultaneously from advanced remote sensing measurements, e.g. multi-spectral polarized sky radiance."

(5) P3, L12. σ_i is the "geometric standard deviation" (not the ordinary one) of r for each mode. As an alternative, if you prefer not introducing the concept of geometric standard deviation, you can say that "lnσ_i is the standard deviation of ln r for each mode".

Response: We have corrected according to the Reviewer's comments.
"C_i (μm^3/μm^2) and r_i (μm) and ln σ_i are the volume modal concentration, median radius and standard deviation of ln r_i for each LNM mode, respectively."

(6) P5, L1. Cite:
J. A. Nelder, and R. Mead (1965), "A simplex method for function minimization". Comp. J., 7, 308-313, doi: 10.1093/comjnl/7.4.308

Response: We have cited the paper according to the Reviewer's comments.
"…, an iterative procedure is performed by minimizing Chi-Square on VPSD (see Eq.5) using the NelderMead simplex algorithm (Nelder and Mead, 1965; Lagarias et al., 1998)."

(7) P9, L1. What does "In a meaning of band average" mean?

Response: "In a meaning of band average" means the RMSE is calculated in each wavelength and the largest RMSE in five wavelength appears in the dust type. We

rewrite the sentence as follows:
"The largest root-mean-square-error (RMSE) of fitting τ appears in the dust type, corResponse to the underestimate of n_f and n_c (Fig. 3)."

(8) P10, L16-17. I do not understand the meaning of the last sentence: "Either sensitivity on τ or τ_a will be able to support the estimation of related sub-CRI parameters".

Response: This is an English expression problem. We replaced the sentence by "this suggest that both τ and τ_a sensitivities contribute to the convergence of the iterative scheme. Given only one information (τ or τ_a) is sensitive, it is still possible to constrain the scheme give its sensitivity is strong enough."

TECHNICAL CORRECTIONS

(1) P2, L16. Consider moving "inventories" before the parenthesis.

Response: We have corrected according to the Reviewer's comments.
"…, aerosols radiative properties are simulated based on source emission inventories (i.e. fine and coarse sources separately), …"

(2) P2, L17. P2, L17. "knowledge of . . . are essential" -> ". . . is essential . . . "

Response: We have corrected according to the Reviewer's comments.
"…, and thus knowledge on CRI of different aerosol modes is essential to validate model performance for the assessment of aerosol climate effects."

(3) P3, L21. "subsequence" -> "subsequent"

Response: We have corrected according to the Reviewer's comments.
"The above assumed spectral properties of sub-CRIs are useful to simplify subsequent procedure and it basically fits current knowledge on aerosol properties."

(4) P5, L26, "an" -> "a"

Response: We have corrected according to the Reviewer's comments.
"e). Find the optimal solution based on a Limited-memory optimization algorithm (BFGS: Broyden–Fletcher–Goldfarb–Shanno) (Zhu et al., 1997) by constraining both $\tau(\lambda)$ and $\tau_a(\lambda)$ with AERONET products."

(5) P5, L28. "achieves" -> is achieved. "If yes" -> "If so"

Response: We have corrected according to the Reviewer's comments.
"Check if the convergence, $(f_i - f_{i+1})/\max(f_{i+1}, f_i, 1) < \eta \times \varepsilon$, is achieved. If so, output the separated sub-CRI parameters, …"

(6) P9, L5. "preform" -> "perform". "access" -> "assess" ?

Response: We have corrected according to the Reviewer's comments.
"In order to evaluate the overall performance of the estimation scheme, we perform numerical experiments to assess errors of output sub-mode CRI parameters related to: …"

(7) P9, L18. "imagery" -> "imaginary"

Response: We have corrected according to the Reviewer's comments.
"The errors caused by uncertainty in VPSD are quite different for real and imaginary parts of CRI."

(8) P10, L16. "Another saying" -> "In other words"

Response: We have corrected according to the Reviewer's comments.
"In other words, this suggest that both τ and τ_a sensitivities contribute to the convergence of the iterative scheme. Given only one information (τ or τ_a) is sensitive, it is still possible to constrain the scheme give its sensitivity is strong enough."

(9) P11, L2-3. "relative" -> "relatively", "presents" -> "present", "high" -> "higher", "in the case" -> "for this case" ?

Response: We have corrected according to the Reviewer's comments.
"Although the relatively low sensitivity to n_f present in DU type, the $\delta\tau/\tau$ is still higher than the sensitivity threshold for this case."

(10) P11, L4. "sensibilities" -> "sensitivities"

Response: We have corrected according to the Reviewer's comments.
"The sensitivities of n_c of all three types are considerably low, …"

(11) P12, L13. ". . . the hygroscopicity . . . are significantly increased" -> ". . . is significantly increased"

Response: We have corrected according to the Reviewer's comments.
"…, this discrepancy suggests that hygroscopicity of fine particles is significantly increased in summer under high humidity condition."

(12) P12, L15-16. Consider removing the parentheses from "(kf and kc)", and

from “(kf;440 and kc;440)”.

Response: We have corrected according to the Reviewer’s comments.
“(iii) In Fig.6c, it can be seen that characteristics of k_f and k_c are similar with that of $k_{f,440}$ and $k_{c,440}$, except for the enlarged seasonal variation amplitude (especially for $k_{c,440}$).”

(13) P14, L5. What does "online" mean in this sentence?

Response: The “online” means “real-time”. We rewrite this sentence as follows:
“…, e.g. the joint extinction, absorption and size distribution observation obtained from measurements in real-time.”

Estimation of aerosol complex refractive indices for both fine and coarse modes simultaneously based on AERONET remote sensing products

Ying Zhang [1], Zhengqiang Li [1], Yuhuan Zhang [2], Donghui Li[1], Lili Qie[1], Huizheng Che[3], Hua Xu[1]

[1]State Environmental Protection Key Laboratory of Satellite Remote Sensing, Institute of Remote Sensing and Digital Earth, Chinese Academy of Sciences, Beijing 100101, China
[2]Satellite Environment Center, Ministry of Environmental Protection, Beijing, 100094
[3]Key Laboratory of Atmospheric Chemistry, Chinese Academy of Meteorological Sciences, Chinese Meteorological Administration

Correspondence to: Prof. Zhengqiang Li (lizq@radi.ac.cn)

Abstract. Climate change assessment, especially model evaluation, needs to know complex refractive indices (CRI) of atmospheric aerosols, separately for both fine and coarse modes. However, the widely used aerosol CRI obtained by the global Aerosol Robotic Network (AERONET), correspond to total-column aerosol particles without separation for fine and coarse modes. This paper establishes a method to separate CRIs of fine and coarse particles based on AERONET ~~aerosol products, including~~ volume particle size distribution (VPSD), aerosol optical depth (AOD) and absorbing AOD. The method consists of two steps. First a multimodal log-normal distribution that best approximates the AERONET VPSD is found. Then the fine and coarse mode CRIs are found by iterative fitting of AERONET AODs to Mie calculations.~~The method consists of VPSD breaking down and sub-mode CRI separation parts and yields spectral CRIs for both fine and coarse modes simultaneously.~~ Numerical experiment shows good performance for typical water-soluble, biomass burning and dust aerosol types and the estimated uncertainties on the retrieved sub-mode CRIs are about 0.11 (real part) and 78% (imaginary part), respectively. One year measurements at AERONET Beijing site are processed and we obtain CRIs of 1.48-0.010i (imaginary part at 440nm is 0.012) for fine mode particles and 1.49-0.004i (imaginary part at 440nm is 0.007) for coarse mode particles, for the period of 2014-2015. Our results also suggest that both aerosol fine and coarse mode CRIs have distinct seasonal characteristics, particularly CRIs of fine particles in winter season are significantly higher than summer, due to possible anthropogenic influences.

1 Introduction

Complex Refractive Indices (CRI) of aerosols, describing scattering and absorption properties of atmospheric particulate matters, are important parameters affecting calculation of short-wave radiative budget and aerosol climate effect. Improving the knowledge on aerosol CRI is of great interests to decrease the uncertainties associated to aerosols in the climate change assessment (Boucher et al., 2013). Since 20th century, direct measurement approaches of CRI of small particles have been developed in the laboratory (e.g. Woo et al, 2013; Mogo et al., 2012; Marley et al., 2001; Patterson et al., 1977; Volz, 1973). As to aerosol particles in the real atmosphere, many studies retrieved CRI of near surface aerosols (e.g. Kostenidou et al., 2007; Malloy et al., 2009; Dinar et al., 2006; McMurry et al., 2002), through in situ measurements of particle size distribution as well as scattering and absorption coefficients. Meanwhile, several remote sensing methods were developed to obtain CRI of total-column atmospheric aerosols (e.g. Raut & Chazette, 2007; Li et al., 2006; Sinyuk et al., 2003; Dubovik and King, 2000; Kaufman et al., 2001, Wendisch and von Hoyningen-Huene, 1994; Nakajima et al., 1983). As Nakajima et al. (1983) and Wendisch and von Hoyningen-Huene (1994) reported, the aerosol CRIs can be retrieved by using spectral aerosol optical depth and diffusely scattered radiances. One of widely recognized CRI remote sensing approach is the statistically optimal estimation method based on Sun/sky-radiometer measurements (Dubovik and King, 2000), which has been successfully implemented in the world-wide Aerosol Robotic Network (AERONET) (Holben et al., 1998, 2001). In addition, Li et al. (2006) further ~~supplemented~~ added the polarized sky radiance measurements to the inversion algorithm ~~,~~ in order to better constrain AERONET CRI retrievals. ~~Raut and Chazette (2007) also synthesized t~~The Lidar measurements are also used to obtain CRI of aerosols ~~confined~~ within planetary boundary layer (Raut and Chazette, 2007).

Although above-mentioned remote sensing methods retrieve CRI of total column aerosols, it still remains a big challenge to obtain CRI simultaneously for different modes (e.g. fine and coarse modes, respectively). CRI of fine and coarse modes may differ significantly, due to different compositions and sources (Marley et al., 2001). For example, fine modes are mainly determined by anthropogenic emission or nucleation process, while coarse modes are dominated by natural sources of wind-blown dust or sea salt (Willeke and Whitby, 1975). As to atmospheric models, e.g. the global

three-dimensional chemical transport model (GEOS-Chem) and the Community Multi-scale Air Quality model (CMAQ), aerosols radiative properties are simulated based on source emission inventories (i.e. fine and coarse sources separately) ~~inventories~~, and thus knowledge on CRI of different aerosol modes ~~are~~ is essential to validate model performance for the assessment of aerosol climate effects. ~~There are o~~Only few studies (e.g. Xu et al., 2015; Wu et al., 2015) attempted to retrieve CRI of both fine and coarse modes simultaneously from advanced ~~ground based~~ remote sensing measurements, e.g. multi-spectral polarized sky radiance. Meanwhile, most of AERONET sites provide official CRI products without distinguishing fine and coarse modes. Considering the essential values of world-wide, long-term continuous and high quality AERONET CRI dataset, it is valuable to develop an approach to separate CRI for both fine and coarse modes, based on directly AERONET official aerosol products, instead of developing an entire algorithm performing retrieval from radiance level.

In this paper, we introduce a method to separate CRI of both fine and coarse modes from AERONET aerosol products (Section 2). Section 3 presents the theoretical simulation and analyses and Section 4 focus on the results of 1-yr measurements in Beijing. The results are summarized in Section 5.

2 Method

The ground-based Sun/sky-radiometer is one of major instrument observing total column atmospheric aerosol properties. There are several long-term Sun/sky-radiometer networks operated regionally or globally, e.g. AERONET (Holben et al., 1998, 2001) and SKYNET (Hashimoto et al., 2012). Several inversion algorithms (e.g. King et al., 1978; Nakajima et al, 1996; Dubovik and King, 2000, 2006; Li et al., 2006) have been developed based on Sun/sky-radiometer to retrieve aerosol parameters, like Aerosol Optical Depth (τ), Single-Scattering Albedo, Absorbing Aerosol Optical Depth (τ_a), Volume Particle Size Distribution (VPSD), real ($n(\lambda)$) and imaginary ($k(\lambda)$) parts of CRI corresponding to total-column atmospheric aerosols. Although VPSD are retrieved for a wide radius range (e.g. 0.05-15 μm) with multi-bins (e.g. 22) showing fine and coarse modes clearly, the n and k parts of CRI are still commonly assumed constant for both fine and coarse modes. In practice, separation of CRI for both fine and coarse modes depends on precisely breaking-down VPSD into individual modes and dealing with spectral variation of CRI. Prior to these key steps, a framework to characterize AERONET aerosol products with both fine and coarse mode is needed to establish.

2.1 Aerosol characterization framework based on AERONET products

In order to separate CRI for different modes, we need to characterize AERONET aerosol products by two major assumptions: (i) AERONET VPSD can be fitted by multi-peak Log-Normal Modes (LNM). We choose multi-modal log-normal distributions to fit the AERONET retrieved VPSD by the following formula:

$$\frac{dV(r)}{dlnr} = \sum_{i=1,m} \frac{C_i}{\sqrt{2\pi}|ln\sigma_i|} exp\left[-\frac{1}{2}\left(\frac{lnr-lnr_i}{ln\sigma_i}\right)^2\right] \quad (1)$$

where dV/dln$r$ (in unit of μm^3/μm^2) is the volume particle size distribution, C_i (μm^3/μm^2) and r_i (μm) and ln σ_i are the volume modal concentration, median radius and standard deviation of ln r_i for each LNM mode, respectively. For most of cases, AERONET VPSD can be separated by two LNMs (i.e. m=2 in Eq. (1)) with fine and coarse modes corresponding to small size and large size peak LNM, respectively. When m is larger than 2, all peaks with radius r_i less than 1.0 μm can be considered as belonging to the fine mode, and others belonging to the coarse mode. (ii) Fine and coarse modes have their own sub-CRIs, while real part (n) of sub-CRIs is spectrally independent, and imaginary part (k) of sub-CRIs have spectral variation follows:

$$n_{f/c}(\lambda) = n_{f/c} \qquad \lambda = 440,675,870,1020\text{nm} \quad (2)$$

$$k_{f/c}(\lambda) = \begin{cases} k_{f/c,440} & \lambda = 440\text{nm} \\ k_{f/c} & \lambda = 675,870,1020\text{nm} \end{cases} \quad (3)$$

where λ denotes standard wavelength of AERONET products, f and c represent fine and coarse modes, respectively.

The above assumed spectral properties of sub-CRIs are useful to simplify ~~subsequence~~ subsequent procedure and it basically fits current knowledge on aerosol properties. Fig.1 shows CRI of various aerosol components, including black carbon, dust, organics, sulfate and aerosol water. Based on these data, CRI real parts (n) of aerosol components are quite constant from UV to near infrared spectral region. Only Hematite, following Sokolik and Toon (1999), shows some spectral variation, but its content is usually very low in aerosols, e.g. less than 5% in mass (Schuster et al., 2015; Wagner et al., 2012; Lafon et al., 2004). In contrast, CRI imaginary parts (k) of aerosol components show significant spectral variation, especially at short wavelengths (e.g. 440 nm). Again, Hematite shows strongly higher absorption at 440 nm so that it can affect k value of entire aerosols although with low concentration. In addition, the imaginary part of organics shows some spectral variation (e.g. a

difference of 0.123 between 350 and 500 nm) while that of black carbon mixture also has a smaller spectral change, e.g. variation of about 0.05 at short wavelength.

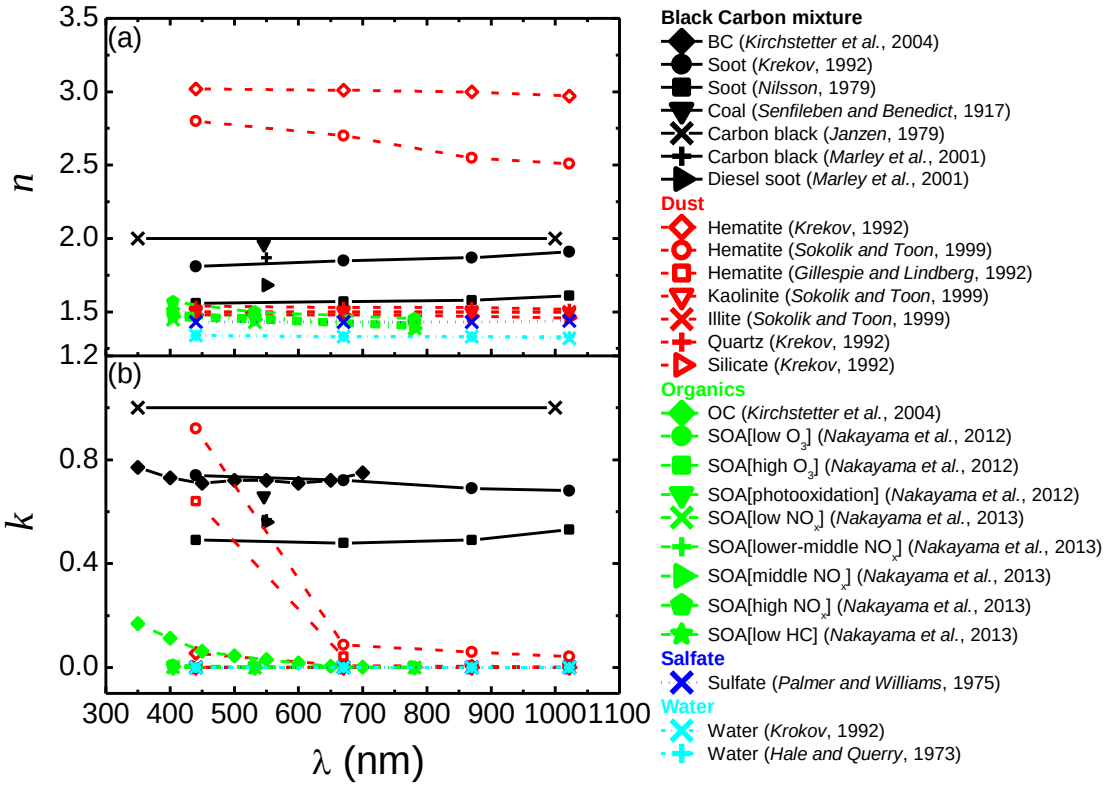

Fig. 1 Complex refractive indices (real part: a; imaginary part: b) reported in literatures. Abbr. BC (Black Carbon), OC (Organic Carbon), SOA (Secondary Organic Carbon).

2.2 Size distribution breaking-down

Optical parameters (e.g. τ and τ_a) of aerosols are usually sensitive to the size distribution and less sensitive to the refractive indices (Zhang et al., 2013; Gobbi et al., 2007). Therefore, the separation of aerosol VPSD is the basis for the next steps of accurate estimation of sub-CRIs. The traditional size distribution breaking-down approaches, e.g. cutting off fine and coarse modes from VPSD based on a fixed or dynamic particle radius, cannot naturally separate fine and coarse modes, especially the obtained sub-mode curve is not a complete log-normal function. Therefore, in this study, we separate the VPSD into complete log-normal functions following the VPSD breaking-down method described in Cuesta et al., (2008). Firstly, we need to set the initial guess values of r_i, σ_i and C_i in Eq. (1). This is based on calculation of the second derivative of VPSD and follows the Eq.4:

$$\begin{cases} g(r) = -\frac{d^2 v(r)}{dr^2} \\ r_i = g^{-1}\left(\max_i\left(g(r)\right)\right),\ i = 1, m \\ \sigma_i = \sqrt{r_i^+ / r_i^-} \\ C_i = v(r_i) \end{cases} \quad (4)$$

where, v (instead of dV/dln$r$) is AERONET VPSD, and r_i^+ and r_i^- are the zero-crossing points of $g(r)$ around r_i in each mode. Then, to obtain the optimized values of these three parameters (i.e. C_i, r_i and σ_i) of each peak, an iterative procedure is performed by minimizing Chi-Square on VPSD (see Eq.5) using the NelderMead simplex algorithm (Nelder and Mead, 1965; Lagarias et al., 1998).

$$\chi^2 = \sum_{j=1}^{22} \frac{\left(v(r_j) - v_{calc}(r_j)\right)^2}{v_{(r_j)}}, \quad j = 1,22 \quad (5)$$

where, v and v_{calc} are dV/dln$r$ from AERONET products and re-calculated from the separated fine and coarse-mode parameters, respectively. And j is the bins of AERONET VPSD.

2.3 Separating refractive indices for fine and coarse modes

According to the aerosol characterization framework in Section 2.1, the flowchart (Fig. 2) of the fine and coarse mode CRI separation is as follows (based on the separated size distribution in Section 2.2):

a). Guesses of 6 output parameters (n_f, $k_{f,440}$, k_c; n_c, $k_{c,440}$, k_c). The initial guess values are set with AERONET product values: $n_f = n_{AERONET}$(440 nm), $k_{f,440}$ and $k_f = k_{AERONET}$(440 nm), $n_c = n_{AERONET}$(870 nm), $k_{c,440}$ and $k_c = k_{AERONET}$(870 nm). Meanwhile, the boundary ranges of these parameters are set as: n_f [1.33, 1.6], n_c [1.33, 1.6], $k_{f,440}$ [0.0, 0.5], $k_{c,440}$ [0.0, 0.5], k_f [0.0001, 0.5] and k_c [0.0001, 0.5].

b). Calculating effective CRI corresponding to each VPSD bins. Here, based on the guessed CRIs of both fine and coarse modes in the previous step, we employ an internal mixing approach, following volume average rule (Heller, 1965), to estimate CRI of each particle radius bins:

$$\begin{aligned} n(r) &= \frac{n_f v_f(r) + n_c v_c(r)}{v_f(r) + v_c(r)} \\ k(\lambda, r) &= \frac{k_f v_f(r) + k_c v_c(r)}{v_f(r) + v_c(r)} \end{aligned} \quad (6)$$

These CRI of each bins can be used to improve the precision of calculation of aerosol optical parameters, employed by next constrain steps.

c). Calculating aerosol optical parameters (τ for λ=440, 500, 675, 870, 1020 nm and τ_a for λ=440, 675, 870, 1020 nm, here wavelengths correspond to AERONET product bands) with the use of the aerosol

CRI and VPSD of step b), by Mie theory:

$$\begin{aligned}\tau(\lambda) &= \int_{0.05}^{15} \pi r^2 Q_{ex}\left(\lambda, r, n(r) - ik(\lambda, r)\right) \cdot \frac{dN(r)}{dr} \cdot dr \\ \tau_s(\lambda) &= \int_{0.05}^{15} \pi r^2 Q_{sc}\left(\lambda, r, n(r) - ik(\lambda, r)\right) \cdot \frac{dN(r)}{dr} \cdot dr \\ \tau_a(\lambda) &= \tau(\lambda) - \tau_s(\lambda)\end{aligned} \quad (7)$$

where dN/dr represents the number size distribution in the atmospheric column which can be pbtained from VPSD, τ_s is the scattering aerosol optical depth, λ is wavelength and r is particle radius. Q_{ex} and Q_{sc}, represent the extinction and scattering efficiency of single spherical particles, respectively.

d). Calculation of Jacobians of $\tau(\lambda)$ and $\tau_a(\lambda)$, by disturbing each sub-CRI parameters by 0.1% (Δ), which is needed by the optimization algorithm in step e).

e). Find the optimal solution based on a~~n~~ Limited-memory optimization algorithm (BFGS: Broyden–Fletcher–Goldfarb–Shanno) (Zhu et al., 1997) by constraining both $\tau(\lambda)$ and $\tau_a(\lambda)$ with AERONET products.

f). Check if the convergence, $(f_i - f_{i+1})/\max(f_{i+1}, f_i, 1) < \eta \times \varepsilon$, is ~~achieves~~achieved. If ~~yes~~so, output the separated sub-CRI parameters, otherwise replace the initial guess with current solution and repeat steps b)-f). Here, f is the Chi-square kernel function, with subscript i and i+1 representing iteration counts, η is a convergence control factor and ε is machine precision (typically setting $\eta = 10^{-4}/\varepsilon$).

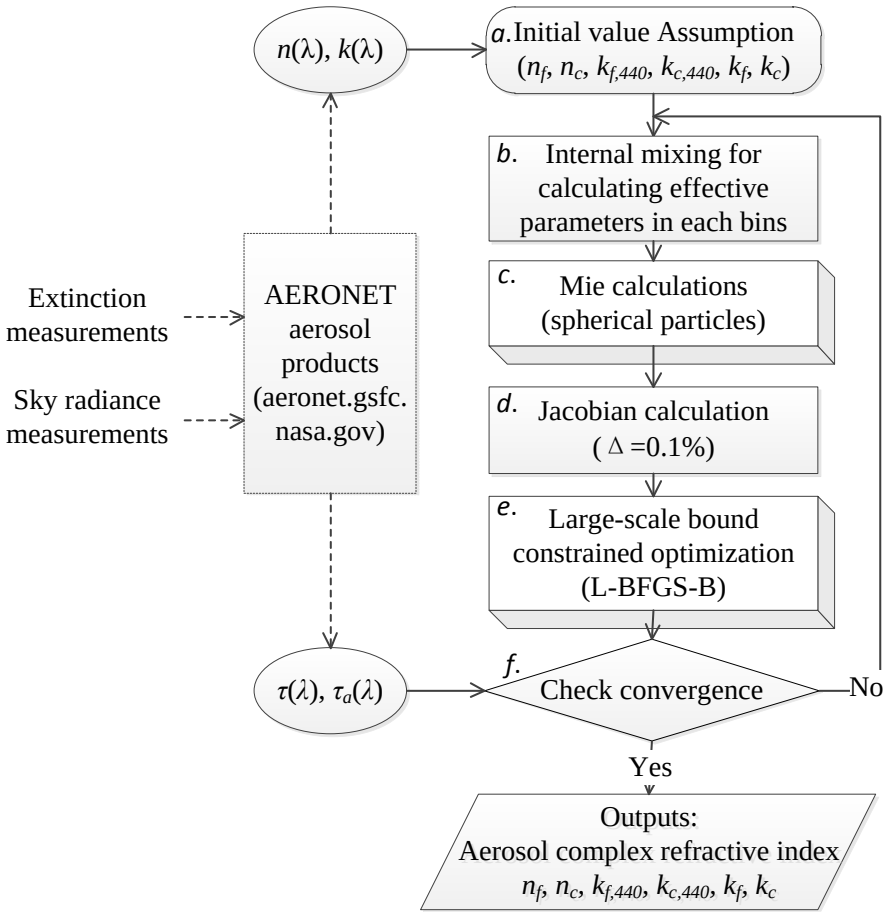

Fig. 2 The flowchart of fine and coarse modes CRI estimation scheme.

3 Numerical tests

3.1 Typical aerosol model test

To test the CRI separation scheme, we employ three typical (i.e. water-soluble, biomass burning and dust) aerosol type models (Table 1) in this paper. These aerosol type parameters are the same with Dubovik et al. (2000), except for supplementing coarse mode n_c and k_c (1.53-i0.008) for all types and keeping original CRIs for only fine modes. Based on these microphysical characters, τ and τ_a (table 1) and diffused sky radiance are calculated by Mie and radiative transfer code. Then, these sky radiance are inverted by AERONET inversion algorithm (Dubovik et al., 2000) to yield AERONET aerosol products (n and k), which will be used as the inputs of our estimation scheme.

Table 1. Typical aerosol models (WS: Water-soluble, BB: Biomass burning, DU: Dust) and their sub-mode parameters.

Type	Fine and coarse mode parameters									AOD & AAOD by Mie		Simulated AERONET products by radiance inversion	
	r_1	r_2	σ_1	σ_2	C_1/C_2	n_f	k_f	n_c	k_c	τ (440/500/675/	τ_a (440/675/	n (440/675/	k (440/675/

										870/1020 nm)	870/1020 nm)	870/1020 nm)	870/1020 nm)
WS	0.118	1.17	0.6	0.6	2	1.45	0.0035	1.53	0.008	0.50/0.41/0.25/ 0.17/0.14	0.02/0.01/ 0.01/0.01	1.45/1.45/ 1.46/1.47	0.0042/0.0039/ 0.0045/0.0047
BB	0.132	4.50	0.4	0.6	4	1.52	0.025	1.53	0.008	0.50/0.39/0.21/ 0.11/0.08	0.06/0.03/ 0.02/0.02	1.52/1.51/ 1.52/1.51	0.0226/0.0199/ 0.0214/0.0216
DU	0.100	3.40	0.6	0.8	0.066	1.53	0.008	1.53	0.008	0.50/0.46/0.40/ 0.38/0.37	0.09/0.07/ 0.06/0.06	1.54/1.51/ 1.52/1.53	0.0085/0.0073/ 0.0089/0.0090

In the numerical test, the initial guess values (see Section 2.3) are set with the bi-modal combined VPSD and (n, k) of the simulated AERONET product (Table 1), additionally with typical errors of AERONET products (i.e. 0.05 in n and 40% in k) (Dubovik et al., 2000), in order to test the scheme tolerance on the initial guess biases. In Fig.3 we present the separated sub-mode CRIs of three typical models and the breaking-down results of VPSD (Fig. 3). It can be seen that both real and imaginary parts of fine and coarse modes are well separated. The maximum error of real part is 0.046 attached to n_c of the biomass burning type, while error of imaginary part is 0.003 for $k_{f,440}$ of the biomass burning. Uncertainty on n_c can be understood as that optical contribution of coarse mode is weak in the case of biomass burning type and thus difficult to be retrieved. Meanwhile, as compensation, the imaginary part k_f is also biased in this case. Moreover, from right column of Fig. 3 we can see that LNM breaking-down are perfectly achieved for each type with very small residuals ($< 6.0\times10^{-5}$) which guarantees the retrieval performance on sub-mode CRIs.

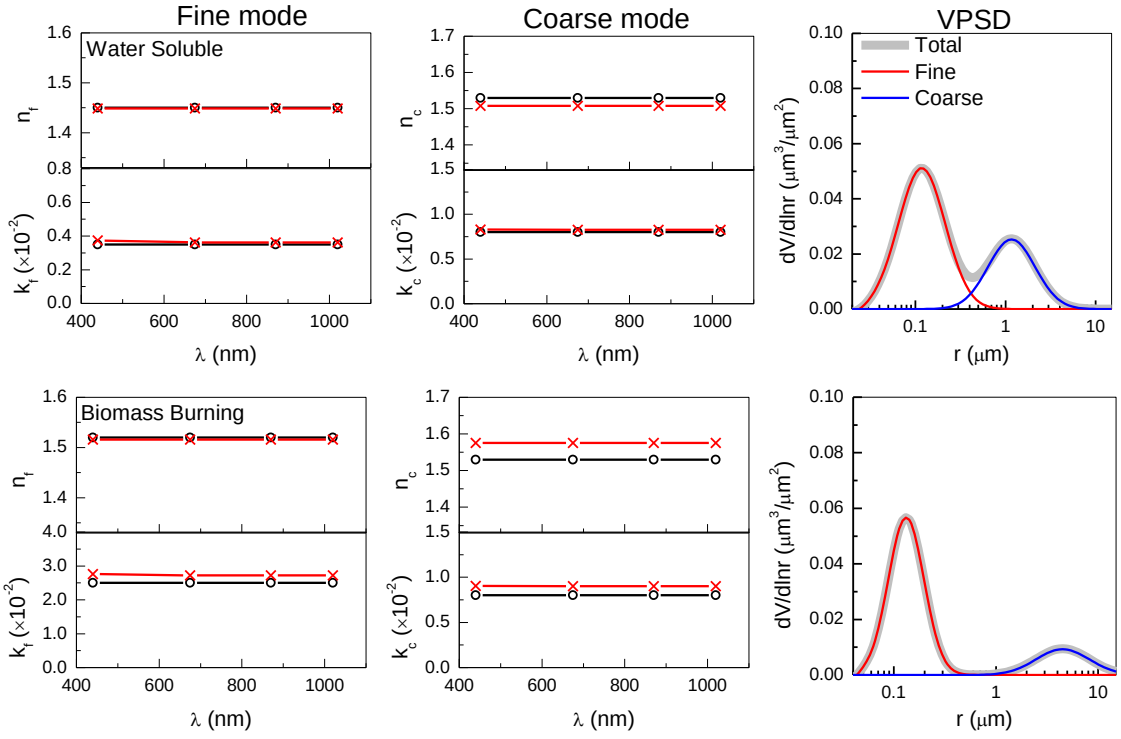

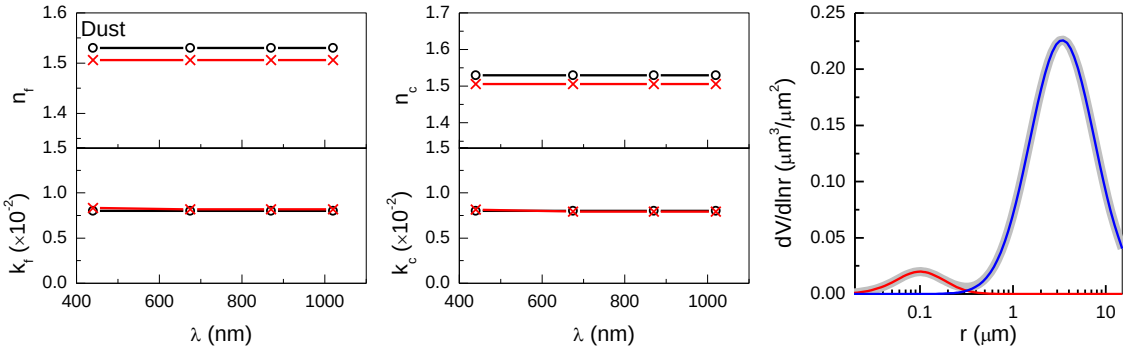

Fig. 3 Estimation of complex refractive indices for both fine (left column) and coarse (middle column) modes of three aerosol types (each row). True values are in circles and retrieved values are in cross symbols. The volume particle size distributions and corresponding breaking-down results (right column) are also shown.

Fig. 4 shows the recovery of τ and τ_a (see step e) of Section 2.3) and comparison with true values listed in table 1. In average, we find fairly good agreements for fitting the spectral τ and τ_a. The absolute τ error of 1.33×10^{-2} at 440nm in dust type, is relatively larger than other wavelengths but still small enough considering that the AERONET AOD measurement uncertainty is about 0.01-0.02. The maximum error on fitting τ_a is about 0.55×10^{-2} corresponding to biomass burning at 440 nm. ~~In a meaning of band average, t~~The largest root-mean-square-error (RMSE) of fitting τ appears in the dust type, corresponds to the underestimate of n_f and n_c (Fig. 3). Similarly, the overestimated $k_{f,440}$ and k_f in the biomass burning type also lead to a relatively larger RMSE (3.34×10^{-3}) on fitting τ_a.

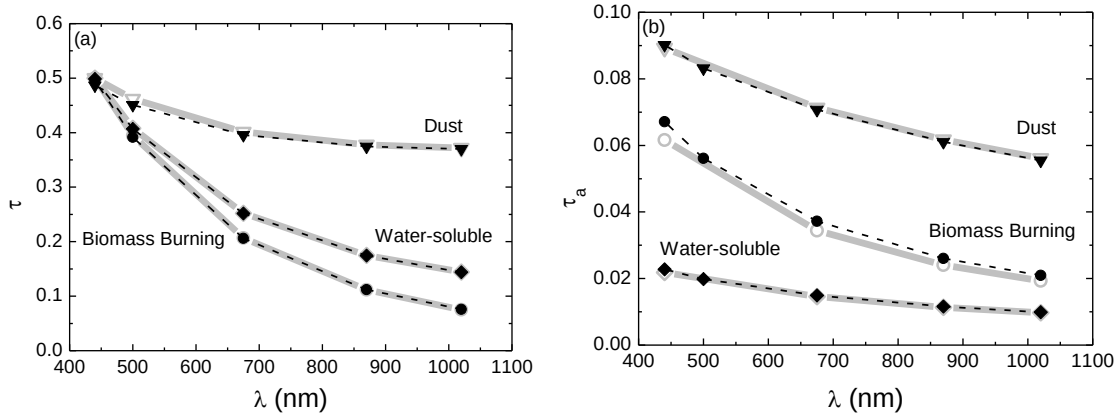

Fig. 4 Recovery of spectral τ (left) and τ_a (right) for three aerosol types (thick line: true, thin line: recovered, corresponding to the separated sub-mode CRIs in Fig.3).

3.2 Error estimation

In order to evaluate the overall performance of the estimation scheme, we p~~r~~erform numerical experiments to ~~access~~ assess errors of output sub-mode CRI parameters related to: (i) uncertainties

on τ. We set typical τ uncertainty (here, 0.01) of AERONET products (Holben et al., 1998; Eck et al., 1999) for all τ bands; (ii) uncertainties on τ_a. Because τ_a of AERONET is obtained by multiplying τ with single-scattering albedo (ω), we consider here ω uncertainty (0.03) of AERONET products (Dubovik et al., 2000) and estimate the uncertainty of τ_a by error propagation; (iii) uncertainties on VPSD. We set 3 typical VPSD (22 bins) uncertainty (15%, 25% and 35% for the average of all bins) of AERONET products following Dubovik et al. (2000) corresponding to the inversion uncertainties on VPSD of water-soluble, biomass burning and dust aerosol type.

Table 2 presents retrieval errors of six sub-mode CRI parameters associated to three typical aerosol types. For the reason of simplification, we only show the impacts of $\Delta\tau$=0.01, $\Delta\omega$=-0.03 and positive error on VPSD, considering that biases caused by input parameter uncertainties are usually symmetric around real values for such kind of retrieval algorithm (Li et al.. 2006). For the influence of $\Delta\tau$ = 0.01, it can be seen that retrieval errors are relatively small. The largest error caused by $\Delta\tau$ = 0.01 is on k_f (dust type) which is 0.0023. As to the influence of $\Delta\omega$ = -0.03, the retrieval errors increase, especially for the imaginary parts, e.g. Δk_c = 0.0074 for water-soluble type. The errors caused by uncertainty in VPSD are quite different for real and ~~imagery~~ imaginary parts of CRI. The retrieval errors of n_f and n_c are larger than those of $k_{f,440}$ and $k_{c,440}$, with the maximum Δn_f of 0.200 in the case of dust type. As a summary of Table 2, considering that it looks like that not all uncertainties reach the maximum simultaneously, and based on error propagation theory, the total uncertainties on the retrieved sub-mode CRI parameters are estimated as Δn_f = 0.106, Δk_f = 50.6% ($\Delta k_{f,440}$ = 75.4%); Δn_c = 0.111, Δk_c = 77.8% ($\Delta k_{c,440}$ = 56.1%), for the average of all typical aerosol types. Or more simplified, the expected errors of sub-mode CRI are $\Delta n_{f/c}$ =0.11 and $\Delta k_{f/c(,440)}$ =78%, which are about 2 times larger than those of AERONET products of all-size CRI (i.e. Δn =0.04 and Δk =40%). This is acceptable and logical considering that we are separating mixed information and these uncertainties are still acceptable for most of applications, e.g. validation of chemical models.

Table 2. Typical uncertainties on the estimated complex refractive indices of fine (*f*) and coarse (*c*) modes. Three error sources (on τ, τ_a and VPSD, respectively) and three aerosol types (WS: water-soluble, BB: Biomass burning, DU: Dust) are considered.

Error sources	Aerosol types	Fine mode			Coarse mode		
		Δn_f	$\Delta k_{f,440}$	Δk_f	Δn_c	$\Delta k_{c,440}$	Δk_c
$\Delta\tau$ = 0.01	WS	0.010	0.0004	0.0003	0.006	0.0009	0.0008
	BB	0.010	0.0001	0.0007	0.044	0.0016	0.0014
	DU	0.026	0.0017	0.0023	0.020	0.0003	0.0002

$\Delta\omega$ = -0.03 (Proxy of $\Delta\tau_a$)	**WS**	0.001	0.0033	0.0001	0.037	0.0066	0.0074
	BB	0.005	0.0073	0.0037	0.046	0.0011	0.0012
	DU	0.008	0.0019	0.0018	0.044	0.0021	0.0026
15 %	**WS**	0.048	0.0007	0.0007	0.1574	0.0032	0.0004
ΔVPSD =25 %	**BB**	0.066	0.0042	0.0045	0.0596	0.0021	0.0021
35 %	**DU**	0.200	0.0072	0.0080	0.0699	0.0024	0.0080
Total error estimation*		0.106	75.41%	50.62%	0.111	56.05%	77.76%

* Total error estimation = $\sqrt{\bar{x}_{\Delta\tau}^2 + \bar{x}_{\Delta\tau_a}^2 + \bar{x}_{\Delta VPSD}^2}$, where $\bar{x}$ represents the mean error of sub-CRIs from three aerosol types.

3.3 Discussion on the sensitivity

As shown in Section 3.1, retrieval performance on the fine and coarse modes can be different with respect to real and imaginary parts of CRI, e.g. for real part, Δn_f is significant less than Δn_c in the case of biomass burning aerosols. This suggests that the natural properties of aerosol modes may affect the accuracy of sub-mode CRI estimation, and thus it is necessary to perform a simple sensitivity study to further clarify the retrieval possibility and possible limitations, besides the numerical error estimation in Section 3.2.

Firstly, we disturb the scheme outputs (e.g. aerosol sub-CRI parameters) by their expected errors (i.e. δn=0.111 and δk=77.7%) as assessed in Section 3.2. Then, by utilizing three aerosol type (WS, BB and DU) models, we trace the effects of these perturbations on the scheme constrain parameters, i.e. τ and τ_a. Finally, we compare these perturbation results ($\delta\tau/\tau$ and $\delta\tau_a/\tau_a$) with their corresponding sensitivity thresholds (e.g. measurement uncertainties), here $\delta\tau/\tau$ = 2% and $\delta\tau_a/\tau_a$ = 6% for AERONET measurements. If the perturbation results are generally beyond the sensitivity thresholds, we can confirm that the constraint parameters are sensitive to the scheme outputs. It should be mentioned that we employ simultaneously τ and τ_a as the constraints in our estimation scheme. In other words, this suggest that both τ and τ_a sensitivities contribute to the convergence of the iterative scheme. Given only one information (τ or τ_a) is sensitive, it is still possible to constrain the scheme give its sensitivity is strong enough. ~~Another saying, either sensitivity on τ or τ_a will be able to support the estimation of related sub-CRI parameters.~~

As illustrated in Fig. 5, we find that τ is mainly sensitive to n_f of the WS and BB types, and their sensitivity curves decrease with the wavelength. Although the relatively low sensitivity to n_f presents in DU type, the $\delta\tau/\tau$ is still higher than the sensitivity threshold ~~in~~ for this~~e~~ case. On the contrary,

sensitivity of k_f increases with wavelength, while much higher sensitivity of k_f embodied in τ_a. The ~~sensibilities~~ sensitivities of n_c of all three types are considerably low, e.g. the largest sensitivity on τ_a is less than 3%. Meanwhile, τ_a is sensitive to both k_c and k_f components except for fine mode of dust type and coarse mode of biomass burning type, with the maximum sensitivity of 43% (k_f of biomass burning). The sensitivity of dust type shows a good qualitative agreement with previous studies (Dubovik et al., 2000; Wendisch and von Hoyningen-huene, 1994).

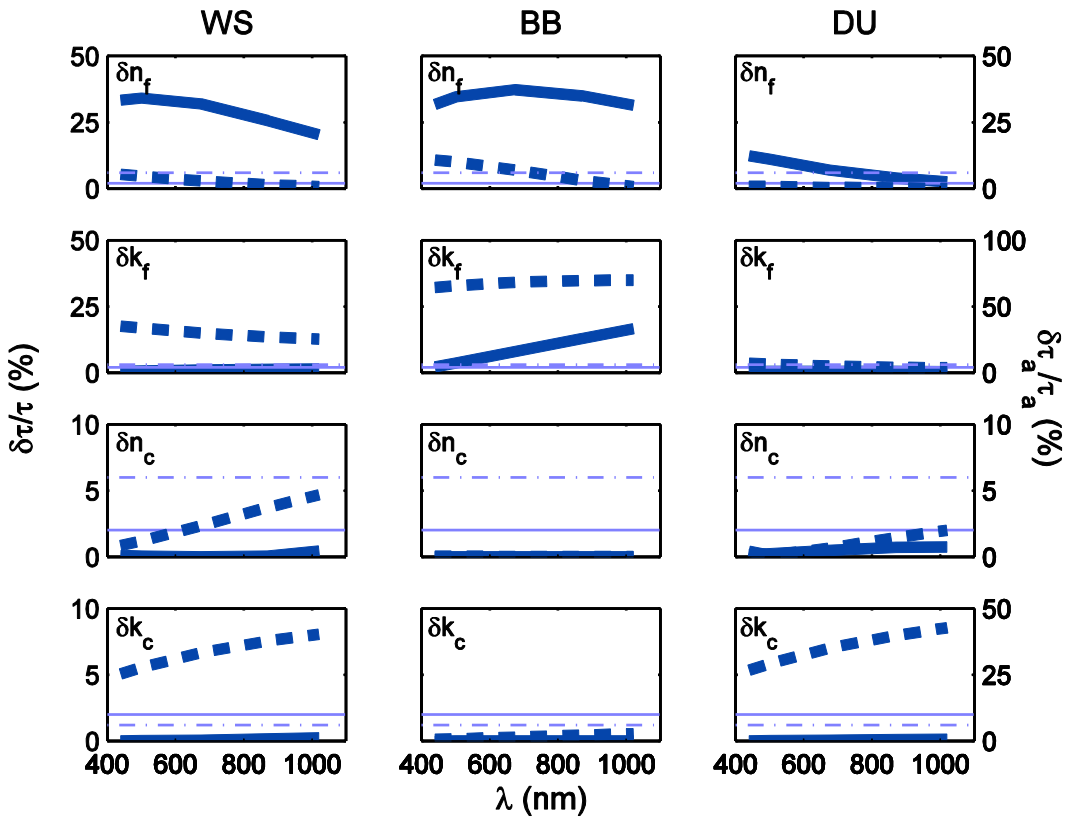

Fig. 5 Sensitivity study on sub-mode CRI parameters (n_f, $k_{f(,440)}$, n_c, $k_{c(,440)}$) to constrain parameters (τ and τ_a) based on three aerosol types (WS: water-soluble, BB: biomass burning, DU: Dust). Thick solid line shows the $\delta\tau/\tau$ and thick dash line shows the $\delta\tau_a/\tau_a$. Thin solid and dash line in figure represent the sensitive thresholds (uncertainty of 2% for τ and 6% for τ_a).

It should be noted that we employ together τ and τ_a and equally weight them in the kernel function of our estimation scheme. Another saying, either sensitivity on τ or τ_a will be able to support the successful estimation of related sub-CRI parameters. Only in the cases that both τ and τ_a have no sensitivity, we will have difficulties in the retrieval. While more accurate initial guess values are expected to decrease the uncertainty, e.g. on n_c suggested by Xu et al. (2015).

4. Test with AERONET Data

The sub-mode CRI estimation scheme can be directly applied to AERONET products. As a realistic test, we chose 1-yr AERONET measurements at Beijing, China, considering its complex aerosol sources and properties resulting from diversified anthropogenic and natural activities. We utilize AERORNET lev 2.0 (data quality assured) data at Beijing CAMS site from Apr. 2014 to Apr. 2015.

The results show that the mean CRI of fine mode in Beijing is 1.48-0.010i (while imaginary part at 440nm is 0.012) and that of coarse mode is 1.49-0.004i (while imaginary part at 440nm is 0.007). These values suggest that fine mode real part refractive index (n_f) are slightly lower than that of coarse mode (n_c), while fine mode imaginary part refractive index (k_f) are greatly higher than that of coarse mode (k_c) in Beijing. Moreover, both fine and coarse modes have larger imaginary parts at 440nm than other wavelengths from 675 to 1020 nm. These results have similar trends as compared with Fig.1 and agree with Hand and Kreidenweis (2002).

For more details, the seasonal mean values of CRIs of fine and coarse modes in Beijing are shown in Fig.6. It can be found that: (i) both n_f and n_c are the lowest in summer (Fig.6a) which agrees with the maximum humidity of summer in Beijing, because higher aerosol water (n=1.33) content tends to decrease real part of CRI. Meanwhile, we found that the discrepancy between n_f and n_c also reaches the maximum in summer. Considering it is generally recognized that coarse particles are weakly hygroscopic, this discrepancy suggests that hygroscopicity of fine particles ~~are~~ is significantly increased in summer under high humidity condition. (ii) For all seasons, k_c is quite constant (Fig.6b). This suggests that large size particulate components are relatively stable in Beijing. In contrast, k_f shows highly seasonal variation and winter value is about 3 times higher than summer, which can be explained by the increase of carbonaceous component emissions during Beijing's winter heating season (Zhang, Jing et al., 2013). (iii) In Fig.6c, it can be seen that characteristics of ~~(k_f~~ and ~~k_c)~~ are similar with that of ~~($k_{f,440}$~~ and ~~$k_{c,440}$)~~, except for the enlarged seasonal variation amplitude (especially for $k_{c,440}$). Compared with Fig.1, we thought that this might be caused by Hematite. As jointly seen with Fig.6b, $k_{c,440}$ decreases significantly in summer which may suggest that the decrease of Hematite is stronger in summer. This indicates some clues on the component changes of coarse particles, e.g. the invaded dust (higher Hematite concentration) might be prohibited significantly in summer due to higher humidity and surface roughness, while the local emission of large particles mainly consist of non-mineral components.

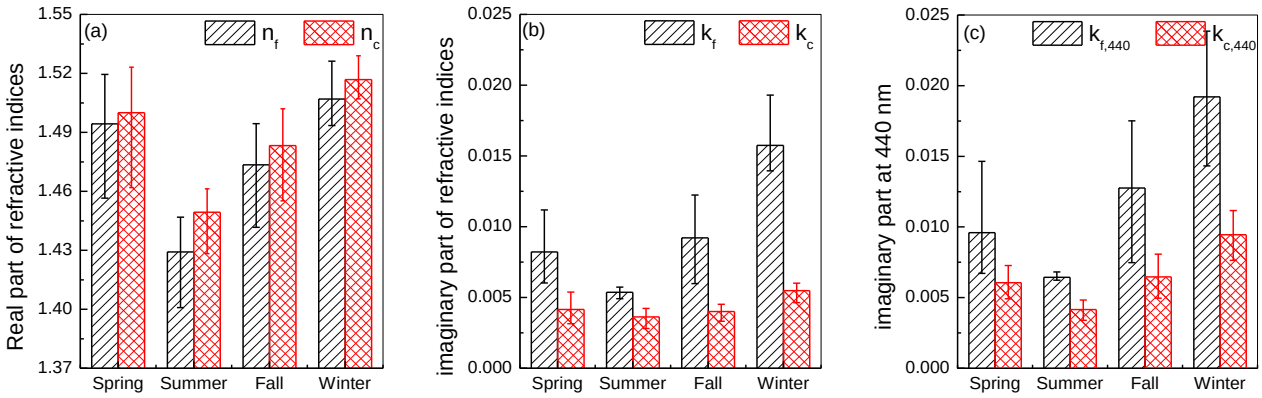

Fig. 6 Seasonal mean of real part (a), imaginary part (b) and imaginary part at 440nm (c) of sub-mode aerosol refractive indices in Beijing 2014-2015. *f* and *c* denote fine and coarse mode respectively. Error bar shows the maximum and minimum of the monthly mean values.

In Fig.7, we illustrate the recovery of scheme input parameters (AERONET τ and τ_a). It can be seen that the maximum averaged bias (relatively 10% and absolutely 0.029) occurs at 1020 nm. Meanwhile the maximum bias (relatively 11% and absolutely 0.002) in τ_a is also attached to this longer wavelength. These biases are basically close to our expectation and claimed uncertainties of AERONET products (τ and τ_a) and thus proves that our sub-mode CRI results are acceptable in the meaning of optical closure.

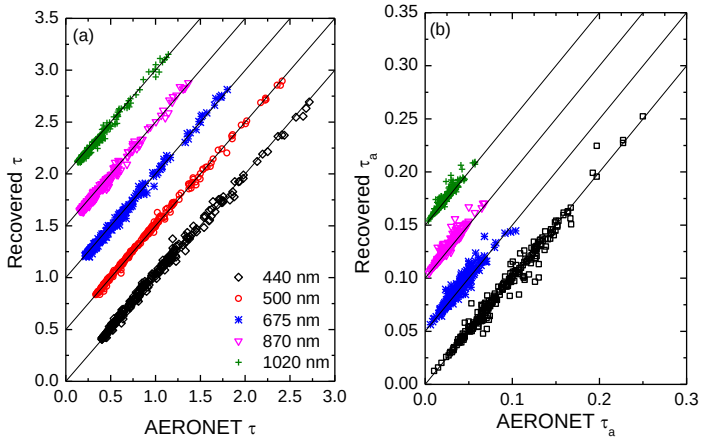

Fig. 7 Recovery of τ and τ_a based on the separated sub-mode aerosol complex refractive indices. N=259 and curves are shifted for a better viewing.

5. Conclusions

This paper establishes a scheme to estimate complex refractive indices of both aerosol fine and coarse modes for the total column atmosphere. The input parameters of the scheme are the volume particle size distribution (VPSD), spectral aerosol optical depth (τ) and absorbing aerosol optical depth (τ_a) of AERONET aerosol products, while AERONET complex refractive indices (CRI)

products are used to generate the initial guesses. The retrieval outputs are aerosol CRIs separated for fine (n_f, $k_{f,440}$, k_f) and coarse modes (n_c, $k_{c,440}$, k_c) simultaneously. We present the VPSD breaking-down and sub-mode CRI iterative inversion techniques as well as the error estimation and test with AERONET real measurements at Beijing site.

The numerical test with three aerosol types shows that sub-mode CRIs can be well retrieved theoretically with the maximum errors less than about 0.046 (real) and 0.003 (imaginary). The total uncertainties on the retrieved CRIs by considering possible input AERONET parameter errors together, are about $\Delta n_{f/c}$=0.11 and $\Delta k_{f/c(,440)}$=78%, respectively. Scheme test based on real measurements are performed in AERONET site in Beijing from 2014 to 2015. The results suggest a CRI of 1.48-0.010i ($k_{f,440}$=0.012) for fine mode particles and 1.49-0.004i ($k_{c,440}$=0.007) for coarse mode aerosol particles. Retrieval results also reveal that CRIs of both fine and coarse particles have distinct characteristic in summer versus other seasons, which is due to difference of hygroscopic effects on fine and coarse particles, as revealed by separated CRI parameters. Meanwhile, results suggest that CRIs of fine particles in winter season, especially the imaginary part, are significantly affected by anthropogenic activities, e.g. carbonaceous components from winter heating.

In the next studies, we will focus on the influence of non-sphericity on dust aerosols, which may help to decrease uncertainties on CRIs of coarse mode particles. In addition, this method is not limited to AERONET remote sensing products and also applicable to in situ measurements, e.g. the joint extinction, absorption and size distribution observation obtained from ~~online instrument~~measurements in real-time.

Acknowledgements. This work was supported by National Natural Science Fund of China (No. 41601386, 91544219, 41671367) and the Chinese Major Project of High Resolution Earth Observation System (30-Y20A39-9003-15/17).

References

Boucher, O., D. Randall, P. Artaxo, C. Bretherton, G. Feingold, P. Forster, V.-M. Kerminen, Y. Kondo, H. Liao, U. Lohmann, P. Rasch, S.K. Satheesh, S. Sherwood, B. Stevens and X.Y. Zhang (2013), Clouds and Aerosols. In: Climate Change 2013: The Physical Science Basis. Contribution of Working Group I to the Fifth Assessment Report of the Intergovernmental Panel on Climate Change [Stocker, T.F., D. Qin, G.-K. Plattner, M. Tignor, S.K. Allen, J. Boschung, A. Nauels, Y. Xia, V. Bex and P.M. Midgley (eds.)]. Cambridge University Press, Cambridge, United Kingdom and New York, NY, USA.

Cuesta J., Flamant P.H., Flamant C. (2008), Synergetic technique combining elastic backscatter lidar data and sunphotometer AERONET inversion for retrieval by layer of aerosol optical and microphysical properties, Appl. Optics., 47, 4598–4611.

Dinar E., Mentel T. F., Rudich Y. (2006), The density of humic acids and humic like substances (HULIS) from fresh and aged wood burning and pollution aerosol particles. Atmospheric Chemistry and Physics, 6(12): 5213-5224.

Dubovik O., Sinyuk A., Lapyonok T., Holben B. N., Mishchenko M., Yang P., Eck T. F., Volten H., Munoz O., Veihelmann B., van der Zande W. J., Leon J. F., Sorokin M. and Slutsker I. (2006), Application of spheroid models to account for aerosol particle nonsphericity in remote sensing of desert dust, Journal of Geophysical Research-Atmospheres, 111(D11), doi: 10.1029/2005JD006619.

Dubovik O. and King M. D. (2000), A flexible inversion algorithm for retrieval of aerosol optical properties from Sun and sky radiance measurements. J. Geophys. Res. Atmos., 105, 20673–20696.

Dubovik O., Smirnov A., Holben B.N., King M.D., Kaufman Y.J., Eck T.F., Slutsker I. (2000), Accuracy assessments of aerosol optical properties retrieved from aerosol robotic network (AERONET) Sun and sky radiance measurements, J. Geophys. Res. Atmos., 105, 9791–9806.

Eck T. F., Holben B. N., Reid J. S., Dubovik O., Smirnov A., O'Neill N. T., Slutsker I., Kinne S. (1999), Wavelength dependence of the optical depth of biomass burning, urban, and desert dust aerosols, J Geophys Res Atmos, 104, 31333–31349.

Gillespie J. B. and Lindberg J. D. (1992), Ultraviolet and visible imaginary refractive-index of strongly absorbing atmospheric particulate matter, Appl. Opt., 31(12), 2112– 2115.

Gobbi, G. P., Kaufman, Y. J., Koren, I., & Eck, T. F. (2007), Classification of aerosol properties derived from AERONET direct sun data, Atmospheric Chemistry and Physics, 7, 453–458.

Hale G. M., and Querry M. R. (1973), Optical-constants of water in 200 nm to 200 mm wavelength region, Appl. Opt., 12(3), 555–563.

Hand J. L. and Kreidenweis S. M. (2002), Anew method for retrieving particle refractive index and effective density from aerosol size distribution data, Aerosol Science and Technology, 36, 1012-1026.

Hashimoto M., Nakajima T., Dubovik O., Campanelli M., Che H., Khatri P., Takamura T., and Pandithurai G. (2012), Development of a new data-processing method for SKYNET sky radiometer observations, Atmos. Meas. Tech., 5, 2723–2737.

Heller, W. (1965), Remarks on refractive index mixture rules, J. Phys. Chem.-Us., 69(4), 1123–1129, doi:10.1021/J100888a006.

Holben B. N. , Tanre D., Smirnov A., Eck T. F., Slutsker I., Abuhassan N., Newcomb W. W., Schafer J. S., Chatenet B., Lavenu F., Kaufman Y. J., Castle J. V., Setzer A., Markham B., Clark D., Frouin R., Halthore R., Karneli A., O'Neill N. T., Pietras C., Pinker R. T., Voss K., Zibordi G. (2001), An emerging ground-based aerosol climatology: aerosol optical depth from AERONET,

J. Geophys. Res. Atmos., 106, 12067–12097.

Holben B. N., Eck T. F., Slutsker I., Tanre D., Buis J. P., Setzer A., Vermote E., Reagan J. A., Kaufman Y. J., Nakajima T., Lavenu F., Jankowiak I., Smirnov A. (1998), AERONET—a federated instrument network and data archive for aerosol characterization, Remote. Sens. Environ., 66, 1–16.

Janzen J. (1979), The refractive index of colloidal carbon, Journal of Colloid and Interface Science, 69:436–447.

Kaufman Y. J., Tanr èD., Dubovik O., Karnieli A., and Remer L. A. (2001), Absorption of sunlight by dust as inferred from satellite and groundbased measurements, Geophys. Res. Lett., 28, 1479–1482.

King M. D., Byrne D. M., Herman B. M. and Reagan J. A. (1978), Aerosol Size Distributions Obtained by Inversion of Spectral Optical Depth Measurements, Journal of the Atmospheric Sciences, 1978(11), 2153-2167.

Kirchstetter T. W., Novakov T., and Hobbs P. V. (2004), Evidence that the spectral dependence of light absorption by aerosols is affected by organic carbon, J. Geophys. Res., 109(D21), D21208, doi:10.1029/2004JD004999.

Kostenidou E., Pathak R. K., Pandis S. N. (2007), An algorithm for the calculation of secondary organic aerosol density combining AMS and SMPS data, Aerosol Science and Technology, 41(11): 1002-1010.

Krekov G. M. (1992), Models of atmospheric aerosols in Aerosol Effects on Climate, edited by S. G. Jennings, pp. 9 –72, Univ. of Ariz. Press, Tucson.

Lafon S., Rajot J.-L., Alfaro S., and Gaudichet A. (2004), Quanlitification of iron oxides in desert aerosol, Atmos. Environ., 38, 1211-1218.

Lagarias J. C., Reeds J. A., Wright M. H., Wright P. E. (1998), Convergence properties of the Nelder–Mead simplex method in low dimensions, SIAM J. Optim., 9(1), 112–147.

Li Z. Q., Goloub P., Devaux C., Gu X., Deuze J-L., Qiao Y., Zhao F. (2006), Retrieval of aerosol optical and physical properties from ground-based spectral, multi-angular, and polarized sun-photometer measurements, Remote Sensing of Environment, 101, 519–533.

Malloy Q. G. J., Nakao S., Qi L., Austin R., Stothers C., Hagino H. and Cocker III D. R. (2009), Real-time aerosol density determination utilizing a modified scanning mobility particle sizer--aerosol particle mass analyzer system, Aerosol Science and Technology, 43(7), 673-678.

Marley N. A., Gaffney J. S., Baird J. C., Blazer C. A., Drayton P. J., and Frederick J. E. (2001), An empirical method for the determination of the complex refractive index of size-fractionated atmospheric aerosols for radiative transfer calculations, Aerosol Sci. Technol., 34, 535–549.

McMurry P. H., Wang X., Park K., and Ehara K. (2002), The relationship between mass and mobility for atmospheric particles: a new technique for measuring particle density, Aerosol Sci. Technol. 36:227–238.

Mogo S., Cachorro V. E., de Frutos A. M. (2012), In situ UV-VIS-NIR absorbing properties of atmospheric aerosol particles: estimates of the imaginary refractive index and comparison with columnar values, Journal of Environmental Management, 111, 267-271.

Nakayama T., Sato K., Matsumi Y., Imamura T., Yamazaki A., and Uchiyama A. (2013), Wavelength and NOx dependence of complex refractive index of SOAs generated from the photooxidation of toluene, Atmospheric Chemistry and Physics, 13, 531-545.

Nakayama T., Sato K., Matsumi Y., Imamura T., Yamazaki A., and Uchiyama A. (2012), Wavelength dependence of refractive index of secondary organic aerosol generated during the ozonolysis and photooxidation of α-pinene, Sola, 8, 119-123.

Nakajima T., Tonna G., Rao R. Z., Boi P., Kaufman Y. and Holben B. (1996), Use of sky brightness measurements from ground for remote sensing of particulate polydispersions, Applied Optics, 35(15), 2672-2686.

Nakajima T., Tanaka M. and Yamauchi T. (1983), Retrieval of the optical properties of aerosols from aureole and extinction data, Applied Optics, 22, 2951-2959.

Nelder J. A. and Mead R. (1965), A simplex method for function minimization, Comp. J., 7, 308-313, doi: 10.1093/comjnl/7.4.308.

Nilsson B. (1979), Meteorological influence on aerosol extinction in the 0.2–40-mm wavelength range, Appl. Opt., 18(20), 3457– 3473.

Palmer K. F., and Williams D. (1975), Optical constants of sulfuric acid -- Application to clouds of Venus, Appl. Opt., 14(1), 208– 219.

Patterson E. M., Gillete D. A., and Stockton B. H. (1977), Complex index of refraction between 300 and 700 nm for Saharan aerosol, J. Geophys. Res., 82, 3153–3160.

Raut J.-C. and Chazette P. (2007), Retrieval of aerosol complex refractive index from a synergy between lidar, sunphotometer and in situ measurements during LISAIR experiment, Atmos. Chem. Phys., 7, 2797–2815.

Schuster, G. L., Dubovik, O., and Arola, A. (2015), Remote sensing of soot carbon – Part 1: Distinguishing different absorbing aerosol species, Atmos. Chem. Phys. Discuss., 15, 13607-13656, doi:10.5194/acpd-15-13607-2015.

Senftleben H., and Benedict E. (1917), Über die optischen Konstanten und die Strahlungsgesetze der Kohle, Annalen der Physik, 54, 65–78.

Sinyuk A., Torres O., and Dubovik O. (2003), Combined use of satellite and surface observations to infer the imaginary part of refractive index of Saharan dust, Geophys. Res. Lett., 30(2), 1081, doi:10.1029/2002GL016189.

Sokolik I. N., and Toon O. B. (1999), Incorporation of mineralogical composition into models of the radiative properties of mineral aerosol from UV to IR wavelengths, J. Geophys. Res., 104(D8), 9423– 9444.

Volz, F. E. (1973), Infrared optical constants of ammonium sulfate, Sahara dust, volcanic pumice,

and fly ash, Appl. Opt., 12, 564-568.

Wagner R., Ajtai T., Kandler K., Lieke K., Linke C., Muller T., Schnaiter M., and Vragel M. (2012), Complex refractive indices of Saharan dust samples at visible and near UV wavelengths: a laboratory study, Atmos. Chem. Phys., 12, 2491-2512.

Wendisch M. and von Hoyningen-Huene W. (1994), Possibility of refractvie index determination of atmospheric aerosol particles by ground-based solar extinction and scattering measurements, Atmospheric Environment, 28(5), 785-792.

Willeke K., Whitby K. T. (1975), Atmospheric aerosols: size distribution interpretation. J. Air. Pollut. Contr. Assoc., 25(5), 529–534.

Woo C., You S., and Lee J. (2013), Determination of refractive index for absorbing spheres, Optik, 124, 5254– 5258.

Wu L.,Hasekamp O., van Diedenhoven B. and Cairns B. (2015), Aerosol retrieval from multiangle, multispectral photopolarimetric measurements: importance of spectral range and angular resolution, Atmos. Meas. Tech., 8, 2625-2638.

Xu, X., Wang J., Zeng J., Spurr R., Liu X., Dubovik O., Li L., Li Z., Mishchenko M. I., Siniuk A., and Holben B.N. (2015), Retrieval of aerosol microphysical properties from AERONET photo-polarimetric measurements: 2. A new research algorithm and case demonstration, J. Geophys. Res. Atmos., 120(14), 7079-7098, doi:10.1002/2015JD023113.

Zhang R., Jing J., Tao J., Hsu S.-C., Wang G., Cao J., Lee C. S. L., Zhu L., Chen Z., Zhao Y., and Shen Z. (2013), Chemical characterization and source apportionment of $PM_{2.5}$ in Beijing: seasonal perspective, Atmos. Chem. Phys., 13, 7053–7074.

Zhang Y., Li Z., Wang Y., Li K., Li D., Zhang Y. H., Wei P., Wang L., Lv Y. (2013), Improving accumulation mode fraction based on spectral aerosol optical depth in Beijing. Spectroscopy and Spectral Analysis, 33, 2795–2802.

Zhu C., Byrd R. H. and Nocedal J. (1997), L-BFGS-B: Algorithm 778: L-BFGS-B, FORTRAN routines for large scale bound constrained optimization, ACM Transactions on Mathematical Software, 23(4), pp. 550 – 560.